4

Crystal Growth: Substructure and Recrystallization

Vadim Glebovsky
Institute of Solid State Physics, the Russian Academy of Sciences
Russia

1. Introduction

Single crystalline refractory transition metals (molybdenum, tungsten, niobium, and tantalum) exhibit a unique combination of properties, namely, high strength, plasticity, Young modulus, wear resistance, number, and low coefficient of linear expansion as well as high radiation resistance which is what makes single crystals of these metals of high purity the most suitable materials to be widely employed in science and engineering. Single crystals of high purity tungsten are well suited to production of the deflectors of the charged particles beams in the linear accelerators, the colliders and, also, to be successfully used as the target-converters for the sources of the positron beams. The attributes of single crystals of molybdenum alloys, compared to their polycrystalline counterparts, include more stable microstructures, lower creep rates, better compatibility with nuclear fuels and lower diffusion penetrability (Liu & Zee, 1996). On the other side, studies of the X-ray wave field in crystals or so called effects of the dynamic scattering theory are of high interest although the first observations of X-ray anomalous transmission are made more than fifty years ago. The necessary high degree of structural perfection is achieved for a limited number of crystals, such as silicon, germanium, and related families; almost no observations of the dynamic effects have been made in metals. Studies of X-ray anomalous transmission in the transition metals are of considerable interest, particularly in tungsten which has a simple structure and a high absorption coefficient.

A method of electron-beam floating zone melting (EBFZM) is widely used to grow single crystals of high-purity refractory transition metals for years (Pfann, 1966; Shah, 1980). The growth of the perfect single crystals of the refractory metals presents difficulties because of the low defect formation energy and the stringent constraints on the level of the temperature gradients. The single crystals of molybdenum and tungsten, grown from the melt by this method, tend to have the specific substructure, characterized by the high dislocation density, reaching 10^5-10^7 cm^{-2}. The main part of these dislocations is collected in the walls, forming the dislocation substructure of the three orders of magnitude. On the one hand, the substructure is due to polygonization of dislocations arising during the growth by one of the known mechanisms (Bolling & Finestein, 1972, Kittel, 1996, Nes & Most, 1966). On the other hand, there is inevitable inheritance of the seed crystal substructure in the growing single crystal, which consists in the fact that the favorably

oriented low-angle boundaries grow up into a crystal. Considerable efforts have therefore been made to improve the structural quality of the tungsten single crystals (Cortenraad *et al*., 2001a). Modern methods of preparing the tungsten single crystals can produce the specimens having the dislocation density of about 10^5 cm^{-2}. A chemical composition, a growth rate, a number of passes by the liquid zone, geometry of the crystals and some other parameters of the growth in varying degrees affect the substructure, but in any case, the substructure of the crystals of molybdenum and tungsten grown from the melt is far imperfect (Glebovsky *et al*., 1988; Glebovsky & Semenov, 1993-1994, 1995, 1999)

However, the single crystals, free of the specific substructure, can be grown by the secondary recrystallization process, which consists of the plastic deformation procedure and the high-temperature annealing procedure. The plastic deformation procedure of monocrystalline specimens can be produced by rolling in the vacuum rolling machines. The high temperature annealing procedure can be performed with the help of the anneal devices inside the rolling machines or in the EBFZM set-ups. The studies of structural perfection of the single crystals grown from the melt and by recrystallization are made by using the methods of X-ray rocking curves and angular scanning topography. To monitor the subgrain substructure of the tungsten single crystals, the X-ray anomalous transmission method has been employed as well. The optimal recrystallization process involves the deformation of single crystals with the [111] growth axis by rolling along the (112) plane. The 6-12% deformation is found to be optimal to get the polycrystals with the large grains of high perfection. The vacuum conditions are most suitable for vacuum rolling to avoid oxidation of the crystal surfaces during deformation at high temperatures. As a result, the single crystals of molybdenum and tungsten have the substructure which is characterized by both the record-low dislocation density and the small mosaic (Glebovsky & Semenov, 1999). For comparison, the tungsten single crystals, grown from the melt, contain the subgrains of the first order, elongated along the growth axis with the misorientation angles of 8-10′ of an arc. The crystallographically perfect tungsten single crystals, obtained by recrystallization, do not contain the subgrains of the first and second orders at all, and the maximum misorientation angles of the subgrains of the third order are less than 1′ of an arc. The structural changes in the perfect single crystals as a result of the thermal stresses, when they have been used as the seed crystals for growing the single crystals from the melt, have been studied.

It is well known that ideal growth techniques and technologies do not exist. All methods and technologies have their own advantages and disadvantages, so the main tasks of researchers consist in developing the advantages and in reducing negative effects of the disadvantages. The EBFZM method has its unique advantages which open wide prospects in the production of the high-purity refractory metals. It would be a mistake if the prospects will not be realized because of the complexities associated with the structural features of the single crystals grown from the melt.

The idea of the chapter is to show the most reliable ways of improving the structural quality of single crystals of the high-purity refractory metals. The recrystallization example for the tungsten single crystals shows how perspective and reliable are these ways in obtaining the structurally perfect single crystals.

2. Brief comments on the electron beam float-zone melting and growing single crystals

Zone-melting techniques (particularly, the EBFZM method) are useful for metals which are very reactive in the liquid state at high temperatures, so they cannot be processed at any contact with other materials (Pfann, 1966). Quoting Pfann, discovered the zone melting technique: "I regard the conception and development of zone melting as an exiting scientific advance. And I cannot help being saddened to hear it occasionally referred to as simply a technical innovation that was mysteriously evoked by the need for transistor grade germanium and silicon. I regard zone melting as elegant both in its simplicity and its surprising complexity." By far the EBFZM method, which is the crucibleless zone melting technique, is characterized by simplicity and complexity, but it is still the best one for melting refractory metals and their alloys. There are some well-known advantages of the method: small volume of the melt; the high efficient EB guns; the well-defined thermal gradients; no contamination from the crucible materials – because instead of them the surface tension of liquid metals works; the non-contaminating way of heating - the electron beams; effective purification which can be achieved due to evaporation of impurities in a vacuum. In parallel, there are some disadvantages of the EBFZM method: it can only be used in a vacuum; limitation of sizes of crystals due to surface overheating and thus decreasing the surface tension of the liquid zone; the high axial temperature gradients in a solid; the high thermal stresses and the high density of the unremovable dislocations; limitation of geometry and mass of the crystals produced by the EBFZM method. These or other properties of the method are marked as the merits or shortcomings, it would be wrong to perceive clearly. Thus, one of the major advantages of the method is absence of refractory crucibles and holding the liquid zone by the surface tension. However, high sensitivity of the surface tension to the surface-active impurities and the temperature gradients converts the recognized advantage into a serious drawback, which prevents growing the single crystals of large diameters, because mass of the liquid zone is too large so that surface tension forces are able to hold it. A similar comment can be done concerning the temperature distribution and the temperature gradients. Certainly, the well-defined thermal gradients are the advantage of the method, but their high values lead to formation of the specific substructure in single crystals, which creates great problems for both the physics research and industrial application. The electronic heating is the really controlled non-contaminating way of heating, but it may only be used in a vacuum, which is also a kind of contradiction when discussing the advantages and the disadvantages of the method.

3. Features of the single crystals growth

The single crystals of the high-purity refractory metals are widely used in modern material science and technology (Alonzo *et al*., 1995; Calverly *et al*., 1957; Glebovsky *et al*., 1998; Hay *et al*., 1968; Liu & Zee, 1996; Moest *et al*., 1998). This necessitates both studying purification processes and developing advanced techniques of growing single crystals of high-purity refractory metals with modern electron beam (EB) guns (M. Cole *et al*., 1968; Glebovsky *et al*., 1986). Crucibleless techniques with electronic heating are extremely important for melting, studying and preparing refractory metals because of their high chemical reactivity in the liquid state. Early zone refining theories such as progressive freezing, zone refining, zone crystal growing, nonideal separation and optimization are studied and discussed

elsewhere (Pfann, 1966; Shah & Wills, 1975). Equipment and technologies such as types of the electron guns used, the drive mechanisms, heating and cooling, floating-zone melting, and stirring are also discussed in detail elsewhere (Shah, 1980). In the EBFZM method the liquid zone is held in place between two vertical collinear solid rods by its surface tension (Fig. 1). Single crystals of high-purity refractory metals can be grown exclusively by EBFZM because of their extremely high melting temperatures and chemical reactivity (Calverly *et al*., 1957; Hay *et al*., 1968; Alonzo *et al*., 1995; Moest *et al*., 1998; Glebovsky *et al*., 1998). This necessitates both studying purification processes and developing advanced methods of growing single crystals metals using modern electron beam guns (M. Cole *et al*., 1968; Glebovsky *et al*., 1986). The main purpose in this field is to study the real structure of single crystals as a function of the technological parameters of the EBFZM method (Langer, 1980; Riedle *et al*., 1994, 1996).

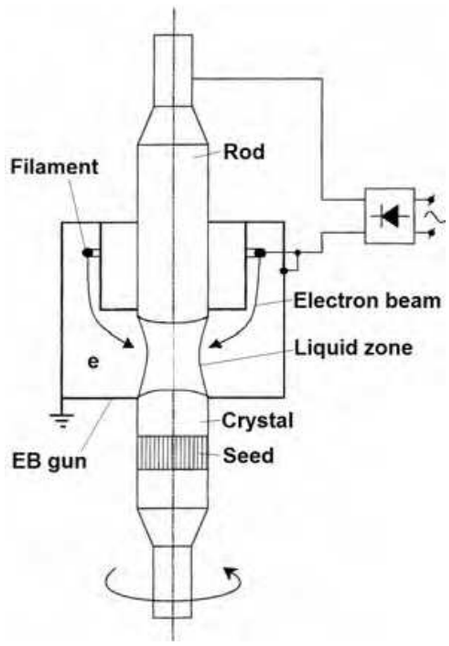

Fig. 1. Thermal zone of the EBFZM.

For effective melting and growing, the original EB guns have been elaborated on because the EB guns is the most important element of the EBFZM set-ups (Glebovsky *et al*., 1986; Shah, 1980). In Fig. 2 the EB gun is shown, which consists of a cathode, an anode, and the focusing electrodes. The main features of the EB gun are: (a) the rod (crystal) serves as the anode, (2) the focusing electrodes made of a water-cooled copper, which makes the EB gun geometrically solid even at very high temperatures in the liquid zone, (3) the focusing electrodes form a stable circular electron beam field and focus it on the liquid zone, (4) the EB gun produces the well-defined thermal gradients on the crystal under the crystallization front. The cathode is made of a circular tungsten filament of 55 mm in dia. An arrangement of the focusing electrodes makes it possible to vary the electron-beam field from a diffuse pattern to sharp one. The advantage of the EB gun is its effectiveness at the refining and growing procedures during service of about 200 hours, compared to the known EB guns which can be used for no longer than 20-30 min. Thus, the original EB gun can be used

continuously, both for refining of refractory metals and growing the single crystals at the growth rates of up to 50 mm/min, diameters up to 35 mm and lengths up to 1100 mm (Glebovsky *et al*., 1986). The growth of single crystals is usually accompanied by purifying liquid metals to high purity. It is demonstrated by preparation of the high-purity refractory metals with the residual impurities at the level of detection of the modern analytical techniques (Alonzo *et al*., 1995; Bdikin *et al*., 1999; Bozhko *et al*., 2008; Chaika *et al*., 2009; Brunner & Glebovsky, 2000a, 2000b; Cortenraad *et al*. 2001a, 2001b, 2001c, 2001d; Ermolov *et al*., 1999, 2002; Glebovsky *et al*., 1998; Markin *et al*., 2006, 2010; Moest *et al*., 1998; Shipilevsky & Glebovsky, 1989). The most problematic metals in growing the single crystals of the refractory metals (molybdenum, tungsten, niobium, and tantalum) are two - molybdenum and tungsten. Therefore, the focus of this chapter is devoted to just these two metals, although almost all the results can be easily applied to other two metals - niobium and tantalum.

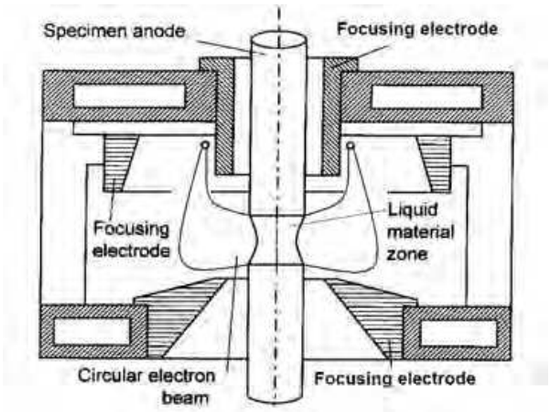

Fig. 2. Circular EB gun with focusing electrodes made of water-cooled copper.

4. Substructure of the molybdenum and tungsten single crystals

Single crystals of refractory metals with the relatively simple *bcc*-lattice grown by EBFZM have the specific dislocation substructure with the size of subgrains, which can be divided into three orders of magnitude. Table 1 shows approximate parameters of the substructures. The chemical composition, especially the content of the interstitial impurities, the growth rate, the number of the liquid zone passes, geometry of the crystal and other parameters significantly affect structural perfection of crystals.

There are several mechanisms of appearance of both the dislocations and substructure of single crystals at growing from the melt (Hurle, 1977; Reid, 1966): under influence of thermal stresses during growing and cooling of single crystals, due to the impurity concentration gradients in the solid phase, due to supersaturating of the lattice with vacancies, inheritance of the substructure of the seed crystal into the growing crystal. In reality, apparently, several mechanisms can operate simultaneously, or some of them will dominate. Obviously, in single crystals of the sufficiently pure refractory metals, effect of impurities on the substructure is unimportant (Akita *et al*., 1973). However, despite of a large number of studies in this area still remain unclearness related with influence of some factors in formation of the substructure.

Order of substructure	Average size of subgrains	Misorientation angles between subgrains
First order	1 mm < d < 8 mm	30′ < θ < 4^0
Second order	50 μm < d < 1 mm	30″ < θ < 30′
Third order	0 < d < 50 μm	0 < θ < 30″

Table 1. Estimated parameters of the crystalline substructure.

In growing the single crystals of molybdenum and tungsten by EBFZM one of the main monitored parameters is the growth rate (or the rate of liquid zone traveling, or the rate of the EB gun displacement). The growth rate is essential both at the crystallization stage, and at the post-crystallization annealing stage, which begins at an interface between the liquid zone and single crystal. At high temperatures, dislocations, regardless of nature of their origin, have very high mobility, so that there polygonization of the dislocation substructure has taken place. Apparently, along with increased dislocation mobility the stresses at the interface between the solid and liquid phases also contribute to formation of the polygonized structure. The typical substructure of the tungsten single crystal with the growth axis [001], revealed at the (010) plane parallel to the growth axis, is shown in Fig. 3. It is clearly seen that the boundaries of the subgrains of the first order extend for the considerable distances along the growth axis. They represent the walls or the dislocation network formed by potential for the *bcc*-lattice dislocations with the Burgers vectors b_1 = a/2 [111] and b_2 = a [100].

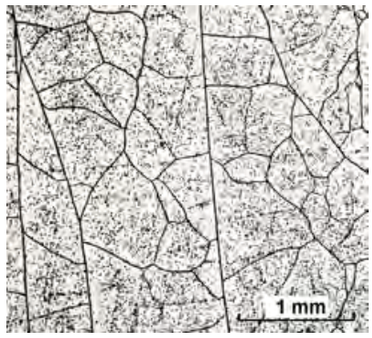

Fig. 3. Substructure of the tungsten single crystal with the vertical growth axis [001] grown at the rate of 2 mm/min. Electrolytic etching in 25% solution of NH_4OH.

The impurities and doping have significant effect on the substructure of single crystals grown from the melt. When microalloying occurs at the definite growth rate, the flat crystallization front is quite stable, and concentration supercooling does not develop. Changes in the dislocation substructure are associated with increase of the dislocation density inside subgrains, decrease of the average size of subgrains and increase of the misorientation angles between subgrains. In the case of doping in significant concentrations, the growth of single crystals becomes impossible at any growth rate. Figure 4 shows the longitudinal and transverse cross-sections of the polycrystalline Mo-2%W alloy, grown from the melt by EBFZM. This polycrystalline ingot contains the large grains elongated along the growth axis. Figure 5 shows the microstructure of the polycrystalline molybdenum ingot of low purity, also grown from the melt by EBFZM. The resulting structure is distinctive: the single-crystalline core surrounded with the polycrystalline periphery.

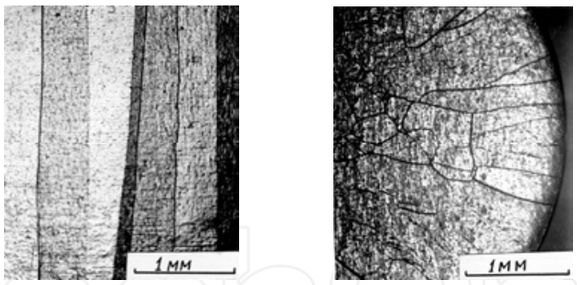

Fig. 4. Microstructure of the polycrystalline Mo-2%W alloy, grown from the melt by EBFZM (longitudinal and transverse cross-sections).

Fig. 5. Microstructure of the polycrystalline molybdenum ingot of low purity, grown from the melt.

To study effect of the growth rate on the substructure, the single crystals of molybdenum and tungsten, having the growth axes along the [001] axis, are grown. The growth rate varied from 0.2 to 50 mm/min, the rotation rate of the growing crystal - from 0 to 100 revolutions per minute. The range of the growth rates under study actually covers all growth rates, implemented in the EBFZM method: the lower limit depends on intense metal evaporation, and the upper limit – by possibility of full melting and stability of the liquid zone. The single crystals are grown in three passes of the liquid zone: the first pass at the growth rate of 6 mm/min, the second pass at the growth rate of 2 mm/min, the third pass - on the seed crystal at the rate from the above range of the rates.

4.1 The substructure of the molybdenum single crystals

The substructures of the molybdenum single crystals vary seriously depending on the growth rate (Glebovsky *et al*., 1988; Glebovsky & Semenov, 1994, 1995; Glover *et al*., 1970, Liu & Zee, 1996). At high growth rates the substructure is characterized by the high dislocation density and the more stressed state. The latter is confirmed by zone annealing the molybdenum single crystal of 8 mm in dia at the temperature close to the melting temperature and at the traveling rate of the EB-gun of 0.5 mm/min. At the low growth rates the dislocations have enough time to be polygonized, because single crystals stay at elevated temperatures for a longer time. Studies of the molybdenum single crystal grown at the growth rate of 6 mm/min show that after zone annealing the crystal has been polygonized to greater extent.

The single crystals grown at the growth rate of 0.5 mm/min have the specific developed substructure with an average size of subgrains of the second order of about 100 μm and the dislocation density, calculated from the etch pits, of $3x10^5$ cm^{-2}. The substructure of the single crystal grown at 6 mm/min is characterized by the individual etch pits and the lack of the polygonized boundaries. The dislocation density is higher - of $1x10^6$ cm^{-2}. The specific substructures of the molybdenum single crystals grown at different growth rates are shown at Fig. 6, 7, and 8. Most clearly the dependence of the misorientation angles of the subgrains on the growth rate is detected by the divergent X-ray beam patterns (Fig. 9). The misorientation angles of the subgrains of the second order in accordance with the value of discontinuities on the line (400) is 50′ of an arc for the growth rate of 0.5 mm/min, and 20′ of an arc – for the growth rate of 6 mm/min.

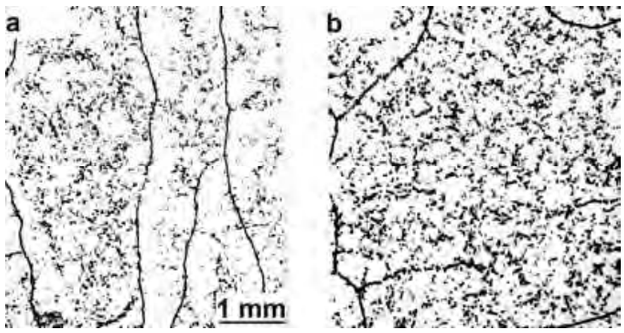

Fig. 6. Specific substructures of longitudinal (a) and transverse (b) cross-sections of the molybdenum single crystal, grown at 2 mm/min.

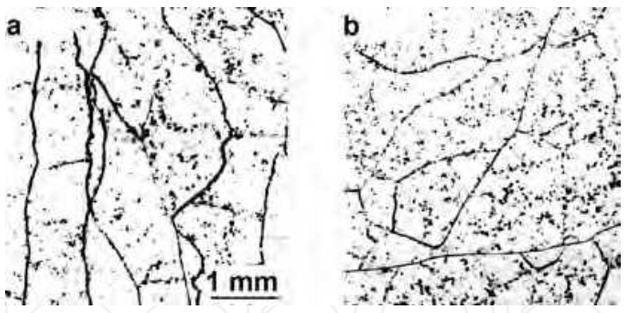

Fig. 7. Specific substructures of longitudinal (a) and transverse (b) cross-sections of the molybdenum single crystal, grown at 10 mm/min

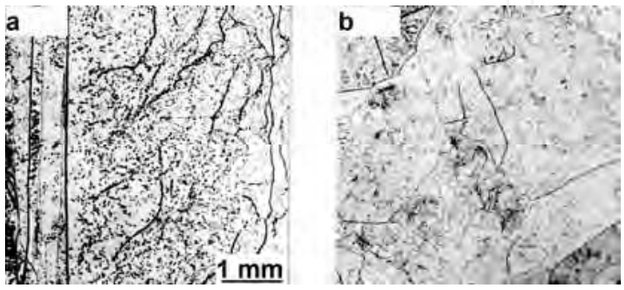

Fig. 8. Specific substructures of longitudinal (a) and transverse (b) cross-sections of the molybdenum single crystal, grown at 40 mm/min.

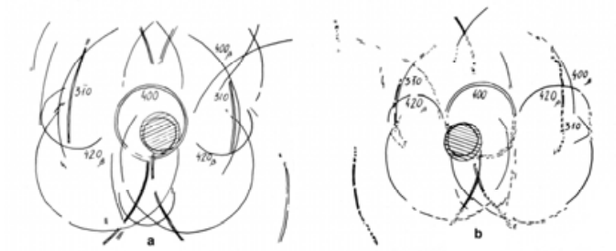

Fig. 9. Divergent X-ray beam patterns of the molybdenum single crystals, grown at rates: a- 0.5 mm/min, b- 6 mm/min.

Another feature of the substructure of the single crystals of molybdenum is radial heterogeneity, detectable at all growth rates. In the central part of the single crystals the boundaries are almost absent; however, at the periphery is observed intense polygonization. Radial inhomogeneity of the single crystals of 8 mm in dia is clearly visible on the divergent X-ray-beams patterns, where the value of shifts at edges of the line (310) is bigger than in the central part: at the edges – 50′ of an arc, in the center – 20′ of an arc. Dependence of nature of the substructure of the single crystals on radial inhomogeneity as well as on the growth rate can be explained by dislocation motion in the non-uniform temperature field of the single crystals.

4.2 The substructure of the tungsten single crystals

The typical substructures of the tungsten single crystals with the growth axis [100] and 10-12 mm in dia, grown at growth rates from 0.5 mm/min up to 40 mm/min, are shown in Fig. 10, 11, and 12. At the growth rates of 0.5-4 mm/min on the transverse cross-sections in the (001) plane, the distribution of the subgrains of the second order by size is close to normal. On the longitudinal cross-sections in the plane (100), pronounced elongated subgrains along the growth axis are found. At 40 mm/min, the polygonization process is not completed: the dislocation density inside the subgrains increases. At two different sites of the tungsten single crystal grown at the growth rates of 2 mm/min and 40 mm/min, the dislocation density increases by a half of an order of magnitude - from $8x10^4$ cm^{-2} to $2x10^5$ cm^{-2}. There is also decrease of the average size of the subgrains, and the misorientation angles are increased to $3\text{-}4^0$ of an arc. Apparently, such influence of the growth rate on the substructure of the tungsten single crystals is common for all refractory transition metals.

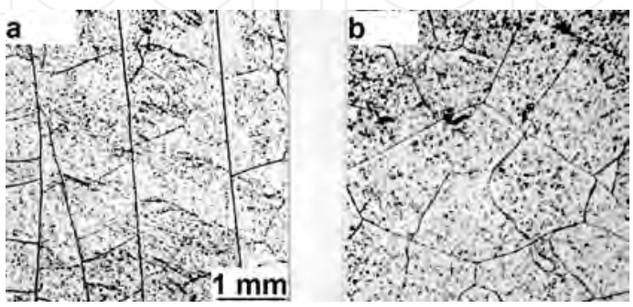

Fig. 10. Specific substructures of longitudinal (a) and transverse (b) cross-sections of the tungsten single crystal grown at 0.5 mm/min.

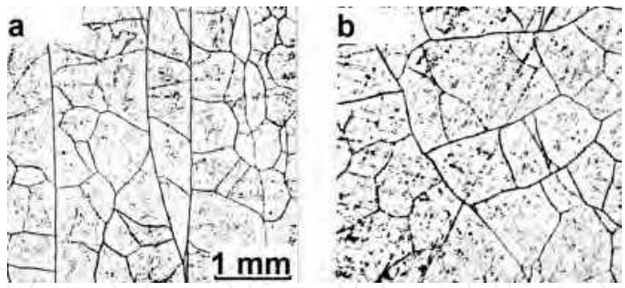

Fig. 11. Specific substructures of longitudinal (a) and transverse (b) cross-sections of the tungsten single crystal, grown at 2 mm/min.

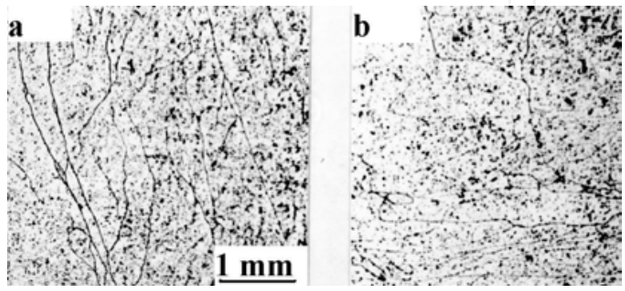

Fig. 12. Specific substructures of longitudinal (a) and transverse (b) cross-sections of the tungsten single crystal, grown at 40 mm/min.

Note significant irregularity of the substructure of the tungsten single crystals in the radial direction: the central part and the periphery are notably different, similar to differences observed in the molybdenum single crystals. The metallographic studies of the substructure of the single crystals of molybdenum and tungsten show that between them there is fundamental similarity. The rate of rotation, and the focusing and power fluctuations of the electron beam, leading to emergence of the constrictions and other defects on the surface of the single crystals, generally have no noticeable effect on the substructure of the single crystals. The fact that the temperature field is non-uniform in the radial direction has been confirmed by existence of the curvilinear crystallization front in vicinity of the seed during zone melting (Fig. 13). In turn, heterogeneity of the temperature field leads to non-uniform mechanical stresses which have different effects on the dislocation motion rate.

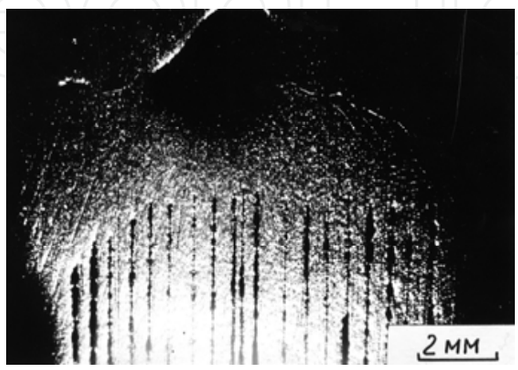

Fig. 13. Macrostructure of the longitudinal thin section of the tungsten single crystal of 11 mm in dia, showing the curvilinear crystallization front in vicinity of the seed.

Although unevenness of the substructure of single crystals creates some problems for physical studies and practical applications (Markin *et al*., 2006, 2010; Mundy *et al*., 1978), there are recent results on successful use of the as-grown single crystals for the manufacture of the STM tips (Bozhko *et al*., 2008; Chaika *et al*., 2009). It is demonstrated the main advantage of the single crystalline W[001] STM tips: sharpness, stability, and the predictable atomic structure. With these tips a set of the complimentary atomically resolved images of the complicated Si(557)5x5 stepped surface reconstruction is reproducibly received and revealed its atomic structure. The example of instability of the W[001] tip illustrates how the known tip axis orientation and the apex atom jump lengths may allow one to predict the atomic structure of the real single crystalline tip that can be of high importance for correct interpretation of the ultimately high resolution STM data. Nevertheless, presence of the specific substructures in single crystals, which prevents expansion of the practical application of single crystals, while insoluble problem for the researchers, that stimulates search for ways of obtaining the perfect single crystals of these metals.

5. Effect of thermal stresses on the substructure of the single crystals

The EBFZM method is characterized by presence of the high axial temperature gradients, especially near the solidification front in both the solid and liquid phases. Since the temperature gradient is a nonlinear function of the distance from the solidification front, *i.e*., $d^2T/dz^2 \neq 0$, this leads to thermal stresses in growing single crystals that can cause multiplication of the dislocations. For a cylindrical crystal with dissipated radiating crystallization heat, the axial temperature gradients can be estimated from the known formulas relating the temperature, the black-body coefficients, the Stefan-Boltzmann constant, the crystal diameter, and thermal conductivity (Table 2).

Metal	The distance from the liquid zone Z, cm						
	0	0,2	0,4	0,6	0,8	1,0	1,2
Molybdenum	-618	-557	-505	-461	-422	-389	-359
Tungsten	-1453	-1207	-1021	-877	-763	-671	-596

Table 2. Axial temperature gradients (K/cm) in the solid state for single crystals of molybdenum and tungsten

The temperature along the axis of single crystals has been measured by optical micropyrometry. The holes of 1 mm in dia and 7-8 mm in depth, located along the axis of the single crystals, serve as a black-body model. Due to the high axial temperature gradients, the black-body model is appeared to be essentially non-isothermal. This increases the temperature measurement error up to $\pm 100^0$, but it is still possible to obtain the reproducible temperature profiles for all metals studied. Figure 14 shows the temperature distribution along the axis of the cylindrical tungsten single crystal of 15 mm in dia. It is seen that near the crystallization front the temperature along the crystal falls particularly sharply to 2000K at 40 mm from the front. The control of the temperature profile along the axis of the liquid zone is performed by measuring an electron current. Owing to the design of the EB gun, the temperature profile of the liquid zone can be effectively changed from diffuse one to sharp, which gives additional opportunity to manage the crystal growth.

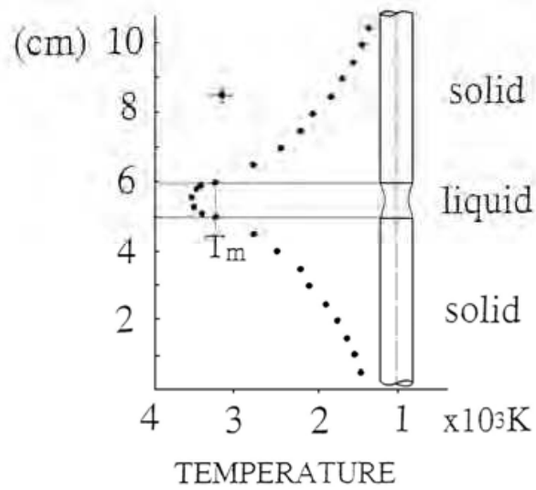

Fig. 14. Temperature distribution along the axis of the cylindrical tungsten single crystal of 15 mm in dia.

For the case of the ax-symmetric temperature distribution along the cylindrical single crystal, resulting thermal stresses are mainly determined by the axial temperature gradients. At pre-melting temperatures, an elastic limit of metals is practically zero and thermal stresses are completely removed by the dislocations, *i.e.*, there is plastic deformation. Since at the growth of crystals from the melt the crystallization heat should released, then inevitably there is the temperature gradient in the solid phase, which leads to the certain density of unremovable dislocations (M. Cole, *et al*., 1961; Buckley-Golder & Hurphreys, 1979; Esterling, 1980; Nes & Most, 1966; Otani, 1984;). The estimate of this dislocation density can be performed by:

$$\rho \geq \alpha \, gradT \, / \, b, \tag{1}$$

Here, α – a linear coefficient of thermal expansion, K^{-1}; *b* - the Burgers vector, cm; *gradT* - the temperature gradient at the crystallization front, K/mm. For tungsten single crystals, such evaluation reveals that in order to have the dislocation density of $\rho = 10^4$ cm^{-2}, the temperature gradient must be less than 50 K/cm. Since the real temperature gradients are usually higher for an order of magnitude, in the melt-grown tungsten single crystals the dislocation density is typically 10^5-10^6 cm^{-2} or even more. The dislocation density in the boundaries is usually for an order of magnitude higher than in the bulk of the subgrains. The estimate by means of the formula (1) with the temperature gradient of 100 K/mm gives the dislocation density of $\rho \geq 5x10^5$ cm^{-2} (Table 3).

Dislocation density ρ, cm^{-2}	Temperature gradients, K/см	
	Molybdenum	Tungsten
10^6	2900	3600
10^5	290	360
10^4	29	36

Table 3. Numerical estimates of temperature gradients at the crystallization front for single crystals of molybdenum and tungsten of 16 and 11 mm in dia, respectively.

Note that dislocations in single crystals are formed under action of thermal stresses in the growth process, and in the cooling process as well. Depending on the cooling rate, the number of the imposed dislocations in the growing crystal can be even higher than the number of the dislocations appeared during the growth (Nes & Most, 1966). The result is in decreasing subgrains sizes, as observed in the thermal shock at welding up both the seed crystal and initial rod together or cutting the crystal by the electron beam. In addition to the axial temperature gradients, quantitative estimates for the stationary stage of the crystal growth have shown, that to form the substructure, the cooling rate is important as well, which is realized in the growing and cooling processes when the crystal growth process is over. For example, in aluminum single crystals obtained by zone melting, the residual dislocation density is of $\rho \sim 10^2$ cm^{-2} when cooled to room temperature at ~ 10^{-3} K/s (about a week), while at the increasing cooling rates on an order of magnitude, the residual dislocation density increases to $\rho \sim 10^4$ cm^{-2}.

In the case of growing the single crystals of molybdenum and tungsten by EBFZM, one can get the estimate from below for the maximum cooling rate of the crystal growth process. The maximum of this magnitude occurs in the solid phase just below the crystallization front. Multiplying the axial temperature gradient on the growth rate, one obtains the value of the maximum cooling rate of the crystal during the growth:

$$\frac{dt}{dz} \times \frac{dz}{dt} = \frac{dT}{dt}. \tag{2}$$

Taking the data of the temperature gradients (Table 3) and the growth rate of 2 mm/min, the most frequently used in practice, one can obtain the cooling rate for molybdenum and tungsten, respectively, 2K/s and 5 K/s, *i.e.,* the cooling rates are very high, taking into account the corresponding values for aluminum (10^{-3} K/s). It should be noted that significant reducing the crystallization rate in the EBFZM method is impossible. The fact that molybdenum and tungsten have very high vapor pressure at $T > T_m$ and at the growth rate of 0.5 mm/min, the metal losses by evaporation can reach 30% of initial mass.

However, even if the crystallization rate tends to zero, desired reduction of the dislocation density still can not be achieved. The reason is that the crystallization rate never coincides with the growth rate (or the rate of the EB gun displacement). In fact, the crystallization rate affects significantly the hydrodynamic processes developing in the liquid zone (Kobayashi, 1970; Kobayashi & Wilcox, 1982; Murphy, 1987; Surek & Chalmers, 1975). These processes give rise to oscillations in the growth rate; moreover, the instantaneous crystallization rate in these moments of time can be significantly greater than the cooling rate, as shown by estimates for molybdenum and tungsten. Presence of such oscillations of both the temperature and growth rate is shown elsewhere (Mullins & Sekerka, 1964; Wilcox & Fuller, 1965). The frequency of these oscillations is close to the inverse of the thermal time constant of the melt-crystal system:

$$f \approx \frac{a}{S} \tag{3}$$

Here, f – a frequency of oscillation, Hz; a – a thermal diffusivity, cm^2/s; S – a cross-sectional area of the crystal, cm^2. Oscillations of the crystallization front in presence of impurities in a

crystal lead to substantial change in the distribution coefficient and, consequently, the so-called transverse striations in the crystals observed by autoradiography.

Considerable interest represents an estimate of the cooling rate from T_m to room temperature. The simplest case can be considered, when the one-dimensional quasilinear heat conductivity equation with the constant coefficients is numerically solved. The process of heat propagation in a homogeneous rod can generally be described by the equation:

$$\rho' C_p \frac{\partial T}{\partial \tau} = \frac{\partial \left(K \frac{\partial T}{\partial X} \right)}{\partial x} + f(x,t) \tag{4}$$

where T (x, t) – a temperature at the point X of the rod at the moment of time t; C_P – heat capacity per unit mass at constant pressure; ρ_m – metal density; K – thermal conductivity; f – density of the heat sources (sinks); X – a coordinate along the rod length L. If one assumes that K, C_P, and ρ' are constant, the equation (4) can be rewritten as:

$$\frac{\partial T}{\partial t} = a^2 \frac{\partial^2 T}{\partial X^2} + f(X,t) \tag{5}$$

Thus, it is necessary to find the continuous solution at $T = T$ (x, t) of the equation (5) for

$$\overline{D} = \{0 \le X \le L; 0 \le t \le t^1\}$$

if

$$T(X,0) = T_0(X); 0 \le X \le L$$
$$T(0,t) = T_1(t); 0 \le t \le t_1$$
$$T(L,t) = T_2(t); 0 \le t \le t_2$$

For a uniform rod with the diameter d, cooling due to radiation and thermal conductivity after switching off the electron beam one obtains instead of the equation (5):

$$\frac{\partial T}{\partial t} = a^2 \frac{\partial^2 T}{\partial X^2} - \frac{4\varepsilon T^4}{d\rho' C_p} \tag{6}$$

In the task the most interesting is the value of $\partial T/\partial t$ with the limitations $0 \le X \le L$; and $t=0$. This value is calculated numerically, and it provides the cooling rate at the upper limit. For these calculations, the following numerical values of the physical parameters are used. For molybdenum: K = 0.909 $Wcm^{-1}K^{-1}$, C_P = 0.235 $Jg^{-1}K^{-1}$, ρ_{Mo} = 10.2 gcm^{-3}, d = 1.6 cm. For tungsten: K = 0.945 $Wcm^{-1}K^{-1}$, C_P = 0.172 $Jg^{-1}K^{-1}$, ρ_W = 19.2 gcm^{-3}, d = 1.1 cm. The cooling rate for molybdenum is $2x10^4$ K/s, and for tungsten – $5x10^4$ K/s. Although these values exceed the cooling rates at the stationary stage of the crystal growth, they can not significantly impact on deterioration of the substructure, because in 5-10 seconds for the most part of the crystal they become comparable with the cooling rates at the stationary phase. The dislocation density can increase only a few in the surface layer near the end of the crystal. Therefore, when the crystals of refractory metals are grown from the melt, it is absolutely impractical to cool slowly, from scientific or technological points of view.

6. Recrystallization of single crystals

Because of relatively low perfectness of single crystals of some semiconductors and refractory metals, grown by EBFZM, there are some studies made to improve the substructure of single crystals. It is well known that the growth of the semiconductor alloys crystals is one of old problems in physics and practice of the crystal growth. The studies on growing such crystals include the casting-recrystallizing-annealing procedures and require careful balancing of the pseudo binary melt stoichiometry, which inherently is a quite difficult process. Increase in recrystallization efficiency can be achieved by adjusting the casting conditions and the suitable thermal gradient during recrystallization (Yadava *et al.*, 1985). This means, that the mechanism of the crystal growth is a combination of both the chemical potential gradient and temperature gradient of zone melting processes, so the growing processes of semiconductor alloys crystals are complicated at their practical realization.

In comparison with the growth of semiconductor crystals, the growth of such simple metals like molybdenum and tungsten seems to be a relatively non-problematic task. However, the main obstacles are both the high melting temperatures and high temperature gradients along single crystals when growing from the melt. Because of these obstacles the growth of single crystals of refractory metals becomes the very complicated task which attracts attention of many scientists for a half a century. Numerous studies concerning this problem have shown that these metals, in spite of their crystallographic simplicity, require special studies, knowledge, and equipment.

Using collected experimental information, the single crystals of molybdenum and tungsten, free of the specific substructure, are produced by recrystallization including plastic deformation and high-temperature annealing (Bdikin *et al.*, 1999; Katoh *et al.*, 1991). Plastic deformation of the crystals has been done by rolling in the vacuum rolling machine or in the standard mills in air. High temperature annealing is produced with the help of the heating devices located inside the rolling machine or in the set-up for electron-beam zone melting and growing single crystals. The comparison of structural perfection of the single crystals grown from the melt and grown by recrystallization is done by both X-ray rocking curves and angular scanning topography.

As a rule, the recrystallized single crystals of molybdenum and tungsten have the substructures characterized by both the record-low dislocation density and small-angle mosaic. It should be noted that the lower dislocation density in the single crystals can only be achieved by recrystallization. As mentioned already before, the optimal procedure involves deformation of the single crystals with the <111> growth axis by rolling along the (112) plane (Bozhko *et al.*, 2008). To monitor both the substructure and perfection of the tungsten single crystals, the anomalous X-rays transmission has been employed as well.

6.1 Experiments on recrystallization of the tungsten single crystals

The tungsten single crystals under study are grown by the EBFZM method (Glebovsky *et al.*, 1986). The single crystals have the different crystallographic growth axes. The high-purity tungsten powders of chemical purity 99.99% are used as a starting material. The as-grown single crystals are 11-22 mm in dia and 100 mm in length. The structural studies involve the X-ray diffraction microscopy methods, namely, angular scanning topography and rocking

curves (Aristov *et al.*, 1974; Bozhko *et al.*, 2008; Brunner & Glebovsky, 2000a, 2000b; Ermolov *et al.*, 1999, 2002; Riedle *et al.*, 1994, 1996).

Several deformation systems are studied, which differ by the crystallographic parameters and strain, because two parameters such as the growth axis and the deformation direction are most important to get the strained single crystals before high-temperature annealing. Crystallographic systems tested are [100]/(010), [100]/(011), [110]/(110), [110]/(111)], [111]/(110) and [111]/(112) where [growth axis]/(rolling plane). The 6-12% deformation by rolling of the two-cant bars with fixed crystallography is found to be optimal to get the large grains. The vacuum conditions are most suitable for the crystal deformation by rolling because they enable one to avoid oxidation of the crystal surfaces during deformation at high temperatures.

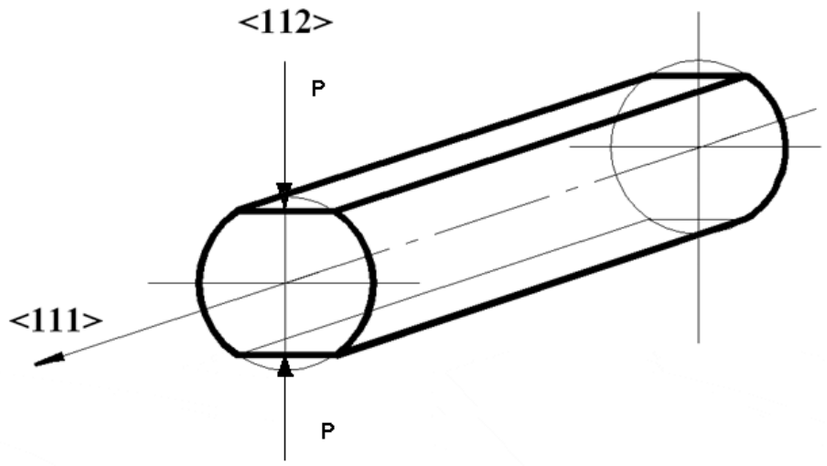

Fig. 15. Two-cants bar with fixed crystallography for rolling. The crystallographic parameters are for the system [111]/(112) where [111] is the growth axis and (112) is the rolling plane (P).

Sample	Growth axis	Rolling plane	Strain, %	Size of grains
1	[100]	(010)	13.4	Grains, 8 mm
2	[100]	(011)	11.6	Grains, 8 mm
3	[100]	(010)	12.3	Grains, 8 mm
4	[100]	(011)	11.6	Grains, 8 mm
5	[110]	(110)	7.9	Grains, 15 mm
6	[110]	(111)	7.5	Grains, 15 mm
7	[111]	(110)	7.5	Grains, 15 mm
8	[111]	(112)	6.6	Grains, 25 mm

Table 4. Parameters of the samples subjected to vacuum rolling followed by high-temperature annealing.

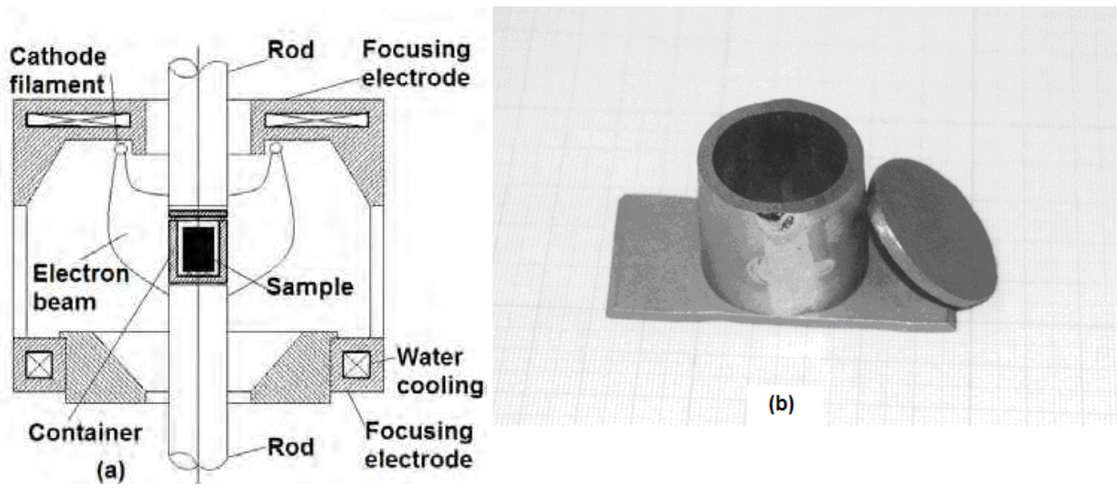

Fig. 16. Electron-beam annealing of a single crystal in a container, a-EB gun, b-container.

The billets to be plastically deformed are produced from the cylindrical tungsten single crystals and have a form of the two-cant bar so that crystallography has been fixed before rolling (Fig. 15). Plastic deformation is performed in one pass at the temperature 900^0C in the vacuum rolling machine or, in a number of cases, in the standard rolling mill in air. In Table 4 are listed the main data for the recrystallized single crystals. The hypercritically strained tungsten single crystals are annealed at 2500^0C in the EBFZM set-up by the defocused electron beam (Fig. 16, a). In order to obtain the more uniform temperature field in the specimens, the tungsten container is used. Its height is 40 mm, the diameter 30 mm, the wall thickness 3 mm (Fig. 16, b). The tungsten specimen of the maximal length 30 mm and the diameter 20 mm is installed inside the container on the tungsten holders. The container has been arranged coaxially with the EB gun equipped with a circular cathode.

6.2 Recrystallized tungsten single crystals in comparison with ones grown from the melt

In order to elucidate influence of recrystallization on the real substructure of tungsten single crystals, the topograms of angular scanning of the specimens, cut from the melt-grown single crystal before deformation, are taken. In Fig. 17, the topograms show the mosaic substructures of two as-grown tungsten single crystals grown in identical conditions. The size of the subgrains is about 1-2 mm, the misorientation angles between subgrains are about 50″ of an arc. On the angular scanning topograms are well seen the small-angle boundaries, their misorientation angles make up tens of the angular minutes, for some single crystals they can exceed 1° of an arc. Single crystals of such structural quality are not suitable for producing, *i.e.*, deflectors and targets using in the runs concerned with channeling of high-energy particles beams. It is necessary to decrease substantially the dislocation density in such crystals and to deplete them from the small-angle boundaries. In contrast to the melt-grown single crystals, necessary structural perfection can only be achieved by the recrystallization processes consisting of plastic deformation and high-temperature annealing.

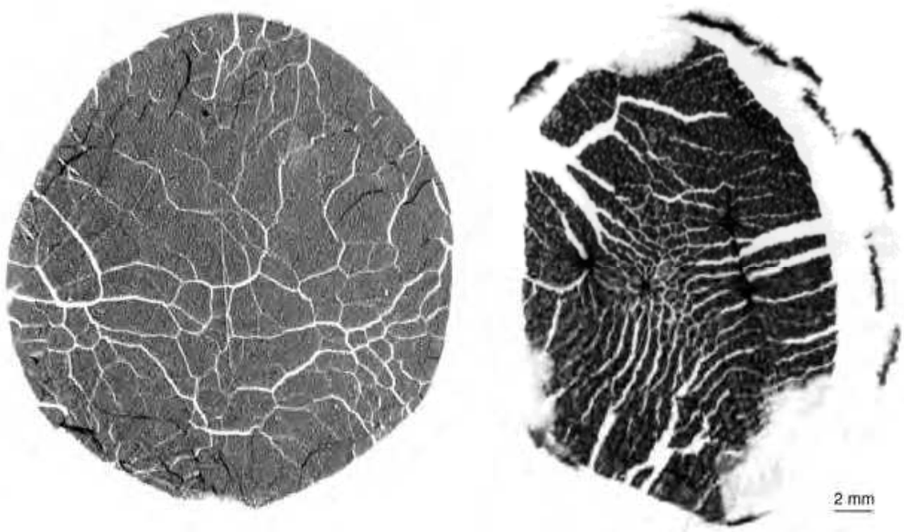

Fig. 17. Angular scanning topograms of two as-grown tungsten single crystals, (110) reflection, CuK_α.

The rocking curves are recorded in the dispersion-free system using the perfect silicon single crystal as a monochromator (Kittel, 1996). To measure the rocking curves, the angle between the X-ray source and the detector is fixed under the first order Bragg diffraction angle. A crystal is rotated with respect to the incoming X-ray beam, and an intensity of the diffracted beam is measured as a function of the angle. The X-ray diffraction rocking curves are measured in three different sites on a specimen surface. The sites differ in a rotation angle of 45^0 in order to exclude texture effects. A half-width (FWHM) of the rocking curves is ~1^0 of an arc. Different subgrains show up as individual peaks on the rocking curves. The angular scanned topograms are obtained in the Θ-2Θ scanning regime and used to study the position, dimensions, and misorientation angles of subgrains. This X-ray diffraction technique is based on a principle of the Bragg reflection (Bdikin *et al.*, 1999; Cortenraad *et al.*, 2001a, 2001b, 2001c, 2001d).

In Table 1 are listed main data for those single crystals. The final recrystallized specimen is the polycrystal incorporating the distinct large grains (Fig. 18). After the recrystallization procedure the large grains do not contain the small-angle boundaries and have the relatively low dislocation density. The optimal procedure, involving deformation of the single crystal with the <111> growth axis by rolling along the (112) plane, is the most suitable for recrystallization. The ~6% deformation is found to be optimal for these crystallographic parameters to get few single nuclei and then large grains to be grown. Higher deformation leads to too many nuclei and as a result - to smaller grains grown. The vacuum conditions are most suitable for rolling because they enable one to avoid oxidation of the crystal surfaces during deformation at high temperatures. By this technique the high purity single crystals of the low dislocation density and free of the small angle boundaries are produced. In several cases the rolled specimens are annealed outside the container. That results in formation of the surface damaged layer of up to 500 μm thick. The middle part of such specimens is virtually free from the small-angle boundaries and has the perfect structure although there are many small subgrains at the periphery.

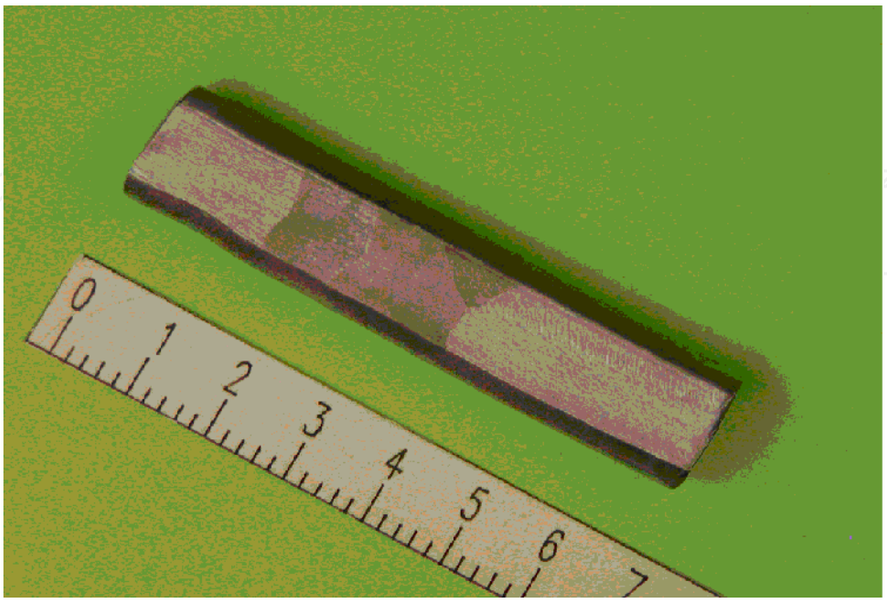

Fig. 18. Recrystallized tungsten polycrystal incorporating three distinct large grains.

Using a tungsten container for high-temperature annealing enables both avoiding damage of the specimen surface layer and decrease of the temperature gradient. The specimens with record structural perfection are obtained by using this technique. The angular scanning topogram and corresponding rocking curve, taken from the specimen annealed in the container are shown in Fig. 19. The angular scanning topogram shows the perfect surface of the specimen, without any boundary or other defects (compare with the topogram for as-grown specimens in Fig. 17). The rocking curve has only one sharp peak with the width at a half height (FWHM) of ~50″ of an arc. Correspondingly, the dislocation density is about $5x10^4$ cm^{-2} for this specimen.

Strong changes of the substructure of the perfect tungsten single crystal has been found when the latter has been used as a seed crystal for growing a new tungsten crystal from the melt by EBFZM (Glebovsky & Semenov, 1999). Before growing, the dislocation density of the seed crystal is of about 10^4 cm^{-1}, and it does not contain any subgrains. After growing from the melt, the substructure of the seed single crystal indicates significant deterioration - subgrains of 500 μm are appeared, and they are elongated along the growth axis with the misorientation angle of 8-10′ of an arc (Fig. 20). At the growth of single crystals of refractory metals from the melt, the main contribution to formation of the substructure is made by the dislocations arising under influence of the thermal stresses during the growth and cooling of the growing crystal. During growing from the melt, dislocations may arise due to thermal stresses in the solid and under action of the impurity concentration gradients due to lattice oversaturation with vacancies. Subgrains are formed by fresh dislocations and walls in spite of the fact that the seed crystal does not contain any subgrains before growing.

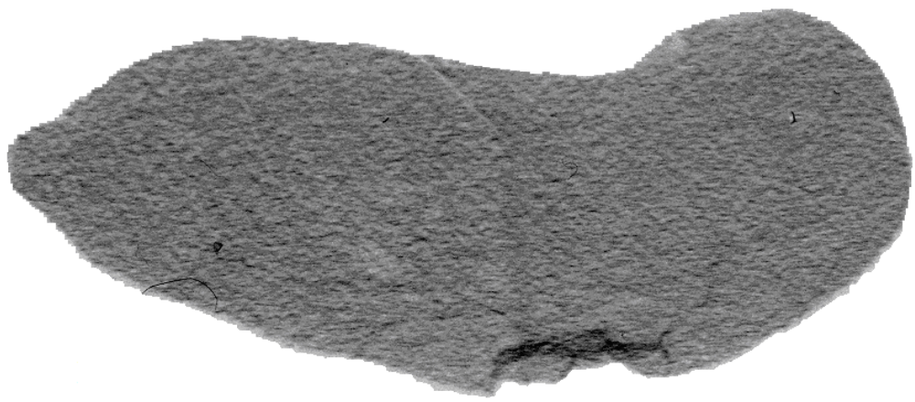

(a)

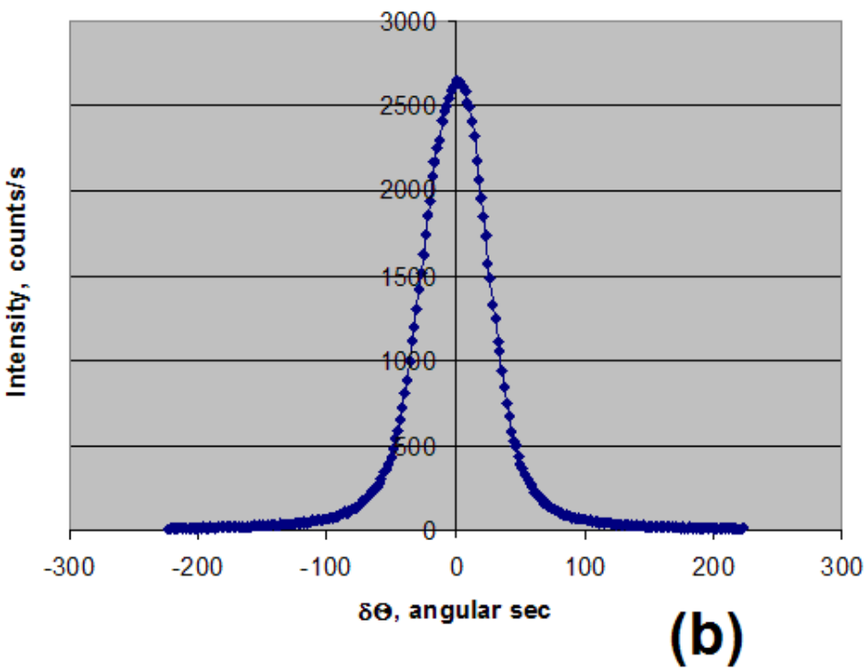

(b)

Fig. 19. Angular scanning topogram (a) and rocking curve (b) of the tungsten single crystal, annealed in the container; the surface plane (110).

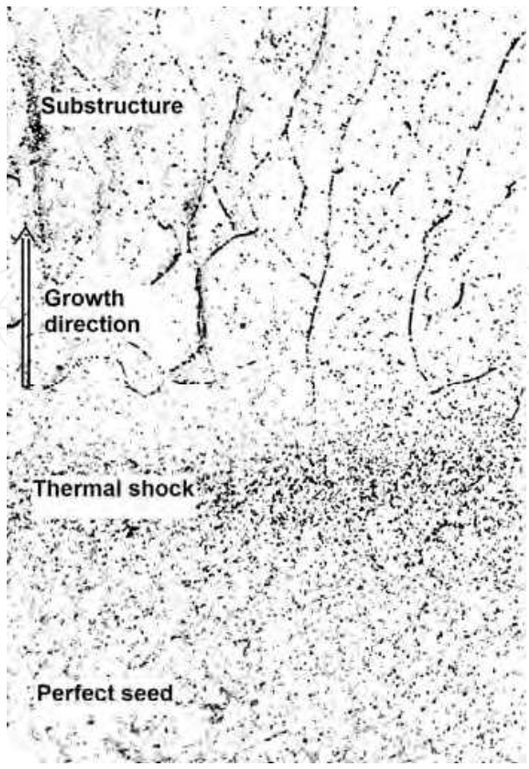

Fig. 20. Appearance of the fresh dislocation walls in the tungsten single crystal during the growth from the melt.

6.3 Anomalous X-ray transmission in the tungsten single crystals

A diverging X-ray beam is the beam where the angles of incidence of the X-rays on the specimen differ for different parts of the specimen (Bdikin *et al*., 1999). Thus, for the given wavelength the diffraction conditions are satisfied along a certain line on the surface of the specimen. The classical system is used to record anomalous X-ray transmission (Borrmann effect). A fine-focus tube with a focus measuring 50x50 μm² is used as a source of the diverging X-ray beam. The distance between the specimen and the photographic film is 10 cm and that between the source and the specimen is 18 cm (Fig. 21). An asymmetric extraction geometry (the distance between the source and the specimen is not equal to that between the specimen and the photographic film) is used to eliminate focusing of the diffracted rays over the radiation spectrum. In the case of dynamic diffraction (perfect crystal) at points, where the diffraction conditions are satisfied, amplification of intensity is observed in the transmitted beam. In kinematic approximation (crystal containing defects), intensity is suppressed. The fact that transmitted radiation is recorded, and radiation intensity is the same in the diffracted and forward transmitted beams, together with observation of amplification of characteristic Cu$K_{\alpha 1,2}$ radiation intensity in these directions indicate that diffraction is of dynamic nature. Observation of splitting of these beams into a Cu$K_{\alpha 1,2}$ doublet (Fig.22) and a shift as the specimen rotates indicate that these beams are of diffraction origin and are not the topological characteristic of the specimen. Diffractometering of the waves which passed in the directions R and T also confirms that intensities of the diffracted and transmitted beams are the same.

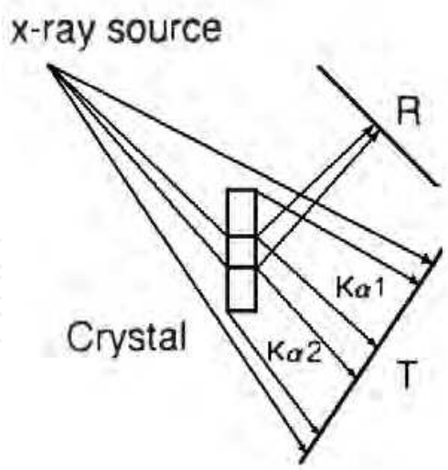

Fig. 21. Scheme for recording the anomalous transmission of X-rays. R-reflection, T-transmission.

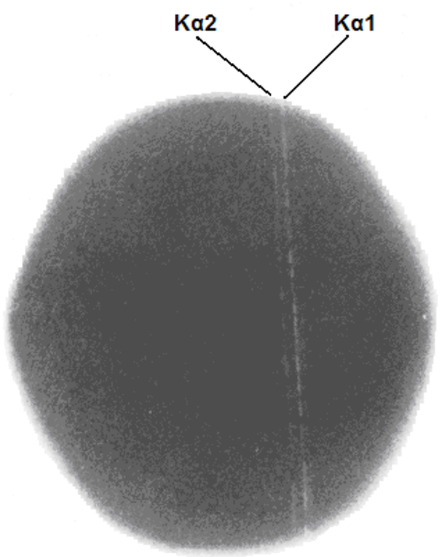

Fig. 22. Anomalous X-rays transmission in a perfect W single crystal; lines are from transmitted beams.

Calculations using the kinematic theory show that for Cu-radiation and the specimen thickness of 0.3 mm (μt ~ 98) absorption is 10^{43}. With the available radiation sources (no more than 10^7-10^8 pulse/s) it is impossible to obtain recordable transmission intensity. For Mo-radiation, absorption is lower than that for Cu-radiation. The linear absorption coefficient of the 0.3 mm thick tungsten single crystal is calculated to be μt = 53.4 on the Mo-radiation characteristics.

If the absorption coefficient is conceived as $\sigma = \mu_i t + y_i$, where μ_i is a coefficient of interference absorption and y_i is responsible for renormalization of the atomic amplitude of scattering, then for the perfect tungsten single crystal can be obtained μ_i = 369.2, y_i = -6.63. The measurements of the absorption coefficient of a diffracted Mo-radiation yield σ = 7.3. Under assumption that y_i is independent of the defects concentration one obtains μ_i =464.3 cm^{-1}, *i.e.,* in the real specimen the interference absorption coefficient is by 25% greater than it has to be in the perfect crystal.

The effects associated with dynamic X-ray propagation can only be observed in crystals for which the distance between the dislocations does not exceed an extinction length *L*. The calculations for (110) CuK_α reflection for the defect-free tungsten crystal give L = 1.7 μm, *i.e.*, the critical dislocation density is $N_d = L^{-2} = 3.5 \times 10^7$ cm^{-2}. From the view point of the specific features of X-ray scattering, the crystal lattice defects fall into two classes. The first class involves localized defects, *e.g*. vacancies, which, virtually, do not deform the reflective atomic planes and, therefore, do not change the rocking curve width. Occurrence of such defects in the crystal only results in decrease of intensity of transmitted radiation, *i.e.,* the growth of the absorption coefficient. The second class involves, for example, dislocations, presence of which gives rise to distortion of the atomic planes and violation of the crystal lattice period. These defects lead to increase of both the angular divergences of the diffracted beam (rocking curve width) and interference absorption coefficient. In the defect-free crystal the waves propagating in the crystal have the finite natural angular width $\delta = \lambda/L$, where λ is the characteristic radiation wavelength.

In order to determine the type of the defects which predominate in the perfect tungsten single crystals and their density, the rocking curves for the (110) reflection in the Bragg and Laue geometries are recorded, and measured the interference damping factor μ_i. In the Laue geometry the width of the rocking curve is 32″ of an arc whereas in the Bragg geometry the width of the rocking curve is 72″ of an arc. The calculated values for these widths in the defect-free crystal are 5.5″ of an arc and 48.6″ of an arc in the Laue and Bragg geometries, respectively. Hence, broadening of the rocking curves in the real crystal compared with the defect-free crystal is around 25″ of an arc for both rocking curves. The difference between the measured values of the rocking curve width and the interference absorption coefficient, and the calculated values for the defect-free crystal can be used to determine the dislocation density N_d in the crystals under study. Estimates of the dislocation density using the width of the rocking curve give $N_d = 2 \times 10^5$ cm^{-2}, and using the interference absorption coefficient – $N_d = 4 \times 10^5$ cm^{-2}. These data show a good agreement with the dislocation density determined using etch pits, $N_d = 5 \times 10^5$ cm^{-2}. Thus, the dislocation density in the real crystal is substantially lower than the critical density. Note that the dislocation density determined from the interference absorption coefficient is higher than that obtained from the rocking curve width. This is evidently attributable to presence of the defects in the crystal (such as the point defects) which increase absorption but make no contribution to the rocking curve width.

The technique used to study the Borrmann effect allows to obtain the angular scanned transmission and reflection topograms for the tungsten crystals, which reveal subgrains larger than 1-2 mm. Comparison of the transmission and reflection topograms suggests that the subgrain substructure exhibits similar reflection but the transmission topograms have a higher image contrast as a result of dynamic narrowing of the diffracted beam for the thick

crystal (the smaller width of the rocking curve in the Laue geometry). The dislocation density determined by the interference absorption coefficient is larger than that determined by the rocking curve width. This is likely due to occurrence of the localized defects in the crystal, for example, the vacancies which virtually do not deform the reflective atomic planes. It is worth mentioning that the reflection topograms include the weak misorientations at the edges which on the transmittance topograms are not manifested since defectness is higher at the crystal edges than in the center. That excludes the effect of anomalous transmission.

The image of the mosaic subgrains is absent on the transmission topograms. This is because the concentration of the defects in the subgrains exceeds the critical concentration $N_d > L^{-2}$, and the regime of dynamic diffraction is not realized in them. Note that in the diffraction direction in the Bragg geometry, the subgrain formation and other structural features, leading to change in the direction of the diffracted beam, are clearly seen on images. This can be attributed to the fact that the distances between the dislocations in such boundaries are less than L and, accordingly, the small-angle boundaries are not transparent from a standpoint of dynamic diffraction that gives rise to the shadowing effect on the topogram.

The obtained results suggest the conclusion about the character of influence of recrystallization on the real structure of the tungsten single crystals. Importantly that effect of anomalous X-ray transmission manifests itself in the subgrains of ~1 mm in size in the as-grown single crystals as well. After recrystallization the sizes of the subgrains having the perfect structure appears to be much larger. In accordance with the dynamic theory of X-ray scattering, the calculated value of FWHM of the rocking curve for the perfect tungsten single crystal is 48″ of an arc. Unfortunately, it is quite difficult to estimate the dislocation density in a limit of small broadening of the rocking curve. Thus, it is possible only to declare - the dislocation density in the tungsten single crystals is very low, about 10^4 cm^{-2}.

7. Conclusions

The dislocation substructure of single crystals of molybdenum and tungsten is characterized by significant similarity and remains virtually unchanged at the growth rates of 0.5-5 mm/min. Significant changes in the substructure, reflected in increasing fragmentation of subgrains and the misorientation angles of up to 3-4^0 of an arc, take place when the growth rates increase to 10-20 mm/min and above. After sudden increase of the growth rates from 2 mm/min to 40 mm/min, the dislocation density inside subgrains increases on an order of magnitude, reaching 5x10^6 cm^{-2}.

Due to the high temperature gradients near the crystallization front and the high cooling rates, the growth of the perfect single crystals of molybdenum and tungsten from the melt is impossible. Even using the perfect seed crystal, free from the small-angle boundaries with the misorientation angles 3′ of an arc, the method does not allow growing crystals of satisfactory structural quality.

The numerical estimates show that the cooling rates of single crystals can reach 10^4 K/s. This results in small increase in the dislocation density in the thin surface layer during cooling, which is quite acceptable. Therefore, to cool single crystals slowly after growing by EBFZM is impractical from all points of view.

The conditions of the growth of single crystals with the ultimately low dislocation density and the small subgrains spread are revealed. The relatively low dislocation density and the lack of the small-angle boundaries are achieved by recrystallization. The optimal procedure involves the 6% deformation of the single crystalline specimen with the <111> growth axis by rolling in vacuum along the <112> plane and *in-situ* high-temperature annealing.

To monitor the subgrain substructure of the tungsten single crystals, the anomalous X-ray transmission method is effective. The Borrmann effect is observed in the recrystallized perfect tungsten single crystals. The dislocation density determined by diffraction data is close to that determined by etch pits (~$5x10^{-4}$ cm^{-2}). This opens potentialities for controlling the dislocation density by the X-ray diffraction techniques. The perfect single crystals can be employed as the novel crystalline deflectors to monitor the beams of relativistic charged particles and for other applications. The recrystallization example shows how perspective and reliable is this way in obtaining structurally perfect single crystals of tungsten and other refractory metals as well.

8. Acknowledgement

The author has a great pleasure to express sincere acknowledgment to my colleagues and friends Valery Semenov, Sergey Ermolov, Eugene Stinov, Sergey Markin, Boris Shipilevsky, and Sergey Bozhko from the Institute of Solid State Physics, Chernogolovka, Russia, for favorable attitude, cooperation in science and life. The author is very grateful to Wolfgang Gust from the Max-Planck Institute fuer Metallforshung, Stuttgart, Germany, to Hidde Brongersma from the Technical University of Eindhoven, Eindhoven, The Netherlands, and to Wayne King from the Lawrence Livermore National Laboratories, Livermore, USA, for fruitful discussions and friendliness for many years. The skillful technical assistance of Victor Lomeyko from the Institute of Solid State Physics, Chernogolovka, Russia, is greatly acknowledged.

9. References

Akita, H., Sampare, D.S., & Flore, N.F. (1973). Substructure control by solidification control in copper crystals. *Metallurgical Transactions*, Vol. 4, pp.1593-1597, ISSN 1073-5623.

Alonzo, V., Berthier, F., Glebovsky, V.G., Priester, L., & Semenov, V.N. (1995). Study of microstructure of a Ni(100) single crystal grown by electron beam floating zone melting. *Journal of Crystal Growth*, Vol.156, pp.480-486, ISSN 0022-0248.

Aristov, V.V., Shmytko, I.M., & Shulakov, E.V. (1974). Application of the X-ray divergent-beam technique for the determination of the angles between crystal blocks. *Journal of Applied Crystallography*, Vol.7, No.4, pp.409-413, ISSN 1600-5767.

Bdikin, I.K., Bozhko, S.I., Semenov, V.N., Smirnova, I.A., Glebovsky, V.G., Ermolov, S.N., & Shekhtman, V.S. (1999). Observation of anomalous transmission of X-rays in tungsten single crystals. *Technical Physics Letters*, Vol.25, No.12, (December 1999), pp.933-935, ISSN 1063-7850.

Bolling, C.F., & Finestein, D. (1972). On vacancy condensation and the origin of dislocations in growth from the melt. *Philosophical Magazine*, Vol.25, No.45, pp.45-66, ISSN 1478-6435.

Bozhko, S.I., Glebovsky, V.G., Semenov, V.N., & Smirnova, I.A. (2008). Study on the growth of tungsten single crystals of high structural quality. *Journal of Crystal Growth*, Vol.311, No.1, pp.1-6, ISSN 0022-0248.

Brunner, D., & Glebovsky, V.G. (2000). The plastic properties of high-purity W single crystals. *Materials Letters,* Vol.42, (February 2000), pp. 290-296, ISSN 0167-577X.

Brunner, D., & Glebovsky, V.G. (2000). Analysis of flow-stress measurements of high-purity tungsten single crystals. *Materials Letters,* Vol.44, (June 2000), pp. 144-152, ISSN 0167-577X.

Buckley-Golder, J.M., & Hurphreys, C.J. (1979). Theoretical investigation of temperature distribution during Chochralski crystal growth. *Philosophical Magazine*, Vol.39, No.1, pp.41-57, ISSN 1478-6435.

Calverly, A., Davies, M. & Lever, R. (1957). The floating-zone melting of refractory metals by electron bombardment. *Journal of Scientific Instruments*, Vol.34, No.4, pp.142-144, ISSN 0950-7671.

Chaika, A.N., Semenov, V.N. Glebovsky, V.G., & Bozhko, S.I. (2009). Scanning tunneling microscopy with single crystalline W[001] tips: High resolution studies of Si(557)5x5 surface. *Applied Physics Letters*, Vol.95, No.17, 173107, ISSN 0003-6951.

Cole, M., Fisher, D.S., & Bucklow, J.A. (1961). Improved electron beam device for zone melting. *British Journal of Applied Physics*, Vol.12, No.10, pp.577-578, ISSN 0508-3443.

Cole, G.S. (1971). Inhomogeneities and their control via solidification. *Metallurgical Transactions*, Vol. 2, pp.357-370, ISSN 1073-5623.

Cortenraad, R.; Ermolov, S.N.; Semenov, V.N.; Denier van der Gon, A.W.; Glebovsky, V.G.; Bozhko, S.I., & Brongersma, H.H. (2001). Growth, characterization and surface cleaning procedures for high-purity tungsten single crystals. *Journal of Crystal Growth,* Vol.222, pp. 154–162, ISSN 0022-0248

Cortenraad, R., Ermolov, S.N., Moest, B., Denier van der Gon, A.W., Glebovsky, V.G. & Brongersma, H.H. (2001). Crystal face dependence of low energy ion scattering signals. *Nuclear Instruments & Methods in Physical Research, B,* Vol.174, pp.173-180, ISSN 0168-9002.

Cortenraad, R., Ermolov, S.N., Denier van der Gon, A.W., Glebovsky, V.G., Brongersma, H.H., Manenschijn, A., Gartner, G., & Belozerov E.V. (2001). Cleaning procedures for single crystal tungsten substrates. *Inorganic Materials,* Vol.37, No.7, pp.673-677, ISSN 0020-1685.

Cortenraad, R., Ermolov, S.N., Semenov, V.N., Denier van der Gon, A.W., Glebovsky, V.G., Bozhko, S.I., Stinov, E.D. & Brongersma, H.H. (2001). Electron-beam growing and purification of W crystals. *Vacuum,* Vol.62, pp.181-188, ISSN 0042-207X.

Ermolov, S.N., Cortenraad, R., Semenov, V.N., Denier van der Gon, A.W., Boghko, S.I., Brongersma, H.H., & Glebovsky, V.G. (1999). Growth and characterization of monocrystalline tungsten substrates. *Vacuum,* Vol.53, pp.83-86, ISSN 0042-207X.

Ermolov, S.N., Glebovsky, V.G., Cortenraad, R., Moest, B., Stinov, E.D., Denier van der Gon, A.W., & Brongersma, H.H. (2002). Low-energy ion scattering by various crystallographic planes of tungsten single crystals. *Physics of Metals & Metallography,* Vol.93, pp.443–449, ISSN 0031-918X.

Esterling, D.M., (1980) Dislocation dissociation in some *bcc*-metals. *Acta Metallurgica*, V.28, pp.1287-1294, ISSN 0956-7151.

Glebovsky, V.G., Lomeyko, V.V., & Semenov, V.N. (1986). Set-up for electron-beam zone melting of refractory materials. *Journal of Less-Common Metals*, Vol.117, pp.385-389, ISSN 0022-5088.

Glebovsky, V.G., Semenov, V.N., & Lomeyko, V.V. (1988) Influence of the crystallization conditions on the structural perfection of molybdenum and tungsten. *Journal of Crystal Growth*, Vol.87, No.1, pp.142-150, ISSN 0022-0248.

Glebovsky, V.G., & Semenov, V.N. (1993-1994), Electron-beam floating zone melting of refractory metals and alloys: art and science. *International Journal of Refractory Metals & Hard Materials*, Vol.12, pp.295-301, ISSN 0263-4368.

Glebovsky, V.G., & Semenov, V.N. (1995). Growing single crystals of high-purity refractory metals by electron-beam zone melting. *High-Temperature Materials & Processes,* Vol.14, pp.121–130, ISSN 0334-6455.

Glebovsky, V.G., Sidorov, N.S., Stinov, E.D., & Gnesin, B.A. (1998). Electron-beam floating zone growing of high-purity cobalt crystals. *Materials Letters*, Vol. 36, August, pp.308-314, ISSN 0167-577X.

Glebovsky, V.G., & Semenov, V.N. (1999). The perfection of tungsten single crystals grown from the melt and solid state. *Vacuum,* Vol.53, pp.71–74, ISSN 0042-207X.

Glover, A.H., Wilcox, B.A., & Hirth, J.P., (1970). Dislocation substructure induced by creep in molybdenum single crystals. *Acta Metallurgica*, V.18, pp.381-397, ISSN 0956-7151.

Hay, D.R., Scogerboe, R.K., & Scala, E. (1968). Electron beam zone purification and analyses of tungsten. *Journal of Less-Common Metals*, Vol.15, No.2, pp.121-127, ISSN 0022-5088.

Hurle, D.T. (1977). Control of diameter in Czochralski and related crystal growth techniques. *Journal of Crystal Growth*, Vol.42, pp.473-482, ISSN 0022-0248.

Katoh, M., Iida, S., Sugita, Y., & Okamoto, K. (1991). X-ray characterization of tungsten single crystals grown by secondary recrystallization method. *Journal of Crystal Growth*, Vol. 112, pp.368-372, ISSN 0022-0248.

Kittel, C. (1996). *Introduction to Solid State Physics* (7th edition), Wiley, New York, USA.

Kobayashi, N. (1977). Power required to form a floating zone and the zone shape. *Journal of Crystal Growth*, Vol.43, pp.417-424, ISSN 0022-0248.

Kobayshi, N., & Wilcox, W.C. (1982). Computational studies of convection in a cylindrical floating zone. *Journal of Crystal Growth*, Vol.59, pp.616-624, ISSN 0022-0248.

Langer, J.S. (1980) Instabilities and pattern formation in crystal growth. *Revue of Modern Physics*, Vol.52, No.1, pp.1-28, ISSN 0034-6861.

Liu, J., & Zee, H.R. (1996). Growth of molybdenum-based alloy single crystals using electron beam zone melting. *Journal of Crystal Growth*, Vol.163, pp.259-265, ISSN 0022-0248.

Markin, S.N., Ermolov, S.N., Sasaki, M., van Welzenis, R., Stinov, E.D., Glebovsky, V.G., & Brongersma, H.H. (2006). Scattering of low-energy ions from the surface of a W(211) single crystal. *Physics of Metals & Metallography*, Vol.102, No.3, pp.274-278, ISSN 0031-918X.

Markin, S.N., Ermolov, S.N., Sasaki, M., van Welzenis, R.G., Glebovsky, V.G., & Brongersma, H.H. (2010). On a peculiarity of low-energy ion scattering from well-ordered *bcc* W(211) surface. *Nuclear Instruments and Methods in Physics Research B.*, Vol.B268, pp.2433-2436, ISSN 0168-9002.

Moest, B., Glebovsky, V.G., Brongersma, H.H., Bergmans, R.H., Denier van der Gon, A.W., & Semenov, V.N. (1998). Study of Pd single crystals grown by crucibleless zone melting. *Journal of Crystal Growth*, Vol.192, pp.410-416, ISSN 0022-0248.

Mullins, W.W., & Sekerka R.F. (1964). Stability of a planar interface during solidification of a dilute binary alloy. *Journal of Applied Physics*, Vol.35, No.2, pp.444-451, ISSN 0021-8979.

Mundy, J.N., Rotman, S.J., Lam, N.Q., Hoff, H.A., & Nowicki, L.J. (1978). Self-diffusion in tungsten. *Physical Revue*, V.B12, No.12, pp.6566-6575, ISSN 1098-0121.

Murphy, Y.A. (1987). Numerical simulation of flow, heat and mass transfer in a floating zone at a high rotational Reynolds numbers. *Journal of Crystal Growth*, Vol.83, No.1, pp.23-34, ISSN 0022-0248.

Nes, E., & Most, W. (1966). Dislocation densities in slow cooled aluminum single crystals. *Philosophical Magazin*e, Vol.13, No.124, pp.855-859, ISSN 1478-6435.

Otani, S., Tanaka, T., & Ishizawa, Y. (1984). Temperature distribution in crystal rods with high melting points prepared by a floating zone technique. *Journal of Crystal Growth*, Vol.66, No.2, pp.419-425, ISSN 0022-0248.

Pfann, W.G. (1966). *Zone Melting* (2nd edition), Wiley, New-York, USA.

Reid, C.N. (1966). Dislocation widths in anisotropic *bcc*-crystals. *Acta Metallurgica*, V.14, pp.13-16, ISSN 0956-7151.

Riedle, J., Gumbsh, P., Fishmeister, Glebovsky, V.G., & Semenov, V.N. (1996). Cleavage fracture and the brittle-to-ductile transition of tungsten single crystals. *Fracture - Instability Dynamics, Scaling, and Ductile/Brittle Behavior*, R.L. Blumberg, J.J. Mecholsky, A.E. Carlsson & E.R. Fuller, eds., Vol.409, pp.23–28, MRS.

Riedle, J., Gumbsh, P., Fishmeister, Glebovsky, V.G., & Semenov, V.N. (1994). Fracture studies of tungsten single crystals. *Materials Letters*, Vol.20, (August 1994), pp.311-317, ISSN 0167-577X.

Shah, J.S., & Wills, H.H. (1975). Zone melting and applied techniques. In: *Crystal Growth*, B.R. Pamplin, ed., Pergamon Press, London, New York, p.194.

Shah, J.S. (1980). Zone refining and its applications (2nd edition). In: *Crystal Growth*, B.R. Pamplin, ed., pp.301-355, Pergamon Press, Oxford.

Surek, T., & Chalmers, B. (1975). The direction of the surface of crystal in contact with its melt. *Journal of Crystal Growth*, Vol.29, No.1, pp.1-11, ISSN 0022-0248.

Shipilevsky, B.M., & Glebovsky, V.G. (1989). Competition of bulk and surface processes in the kinetics of hydrogen and nitrogen evolution from metals into vacuum. *Surface Science,* Vol.216, pp.509–527, ISSN 0039-6028.

Wilcox, W.R., & Fuller, L.D. (1965). Turbulent free convection in Czochralski crystal growth. *Journal of Applied Physics*, Vol.36, pp.2201-2205, ISSN 0021-8979.

Yadava, R.D.S., Sinha, S., Sharma, B.B., & Warrier, R. (1985). Grain growth mechanism during recrystallization of a tellurium rich $Hg_{1-x}Cd_xTe$ cast. *Journal of Crystal Growth*, Vol.73, No.2, pp.343-349, ISSN 0022-0248.

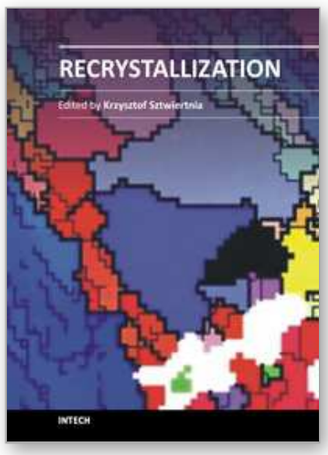

Recrystallization

Edited by Prof. Krzysztof Sztwiertnia

ISBN 978-953-51-0122-2
Hard cover, 464 pages
Publisher InTech
Published online 07, March, 2012
Published in print edition March, 2012

Recrystallization shows selected results obtained during the last few years by scientists who work on recrystallization-related issues. These scientists offer their knowledge from the perspective of a range of scientific disciplines, such as geology and metallurgy. The authors emphasize that the progress in this particular field of science is possible today thanks to the coordinated action of many research groups that work in materials science, chemistry, physics, geology, and other sciences. Thus, it is possible to perform a comprehensive analysis of the scientific problem. The analysis starts from the selection of appropriate techniques and methods of characterization. It is then combined with the development of new tools in diagnostics, and it ends with modeling of phenomena.

How to reference

In order to correctly reference this scholarly work, feel free to copy and paste the following:

Vadim Glebovsky (2012). Crystal Growth: Substructure and Recrystallization, Recrystallization, Prof. Krzysztof Sztwiertnia (Ed.), ISBN: 978-953-51-0122-2, InTech, Available from: http://www.intechopen.com/books/recrystallization/crystal-growth-substructure-and-recrystallization

INTECH
open science | open minds

InTech Europe
University Campus STeP Ri
Slavka Krautzeka 83/A
51000 Rijeka, Croatia
Phone: +385 (51) 770 447
Fax: +385 (51) 686 166
www.intechopen.com

InTech China
Unit 405, Office Block, Hotel Equatorial Shanghai
No.65, Yan An Road (West), Shanghai, 200040, China
中国上海市延安西路65号上海国际贵都大饭店办公楼405单元
Phone: +86-21-62489820
Fax: +86-21-62489821

IntechOpen